ACS APPLIED MATERIALS & INTERFACES

Research Article

www.acsami.org

Template-Activated Strategy toward One-Step Coating Silica Colloidal Microspheres with Sliver

Ke Wang, Xiaoli Zhang, Chunyu Niu, and Yongqiang Wang*

Key Laboratory for Special Functional Materials of the Ministry of Education, Henan University, Kaifeng 475004, P. R. China

Supporting Information

ABSTRACT: Template-activated strategy was developed to coat silica (SiO_2) colloidal microspheres with silver in one step, based on one-pot hydrothermal treatment of silver nitrate, PVP (poly(vinyl pyrrolidone)), and SiO_2 colloidal microspheres in ammonia solution. In our reaction system, the surface of SiO_2 colloidal microspheres was continually activated with negative-charged SiO^- groups in ammonia solution, which accumulated $[Ag(NH_3)_2]^+$ or Ag^+ ions around the SiO_2 colloidal microspheres through electrostatic attraction; thereafter these ions could be reduced into Ag nanoparticles in situ by the weak reducer PVP in the solution, and then acted as seeds for the subsequent complete silver coating with the reaction proceeding. Therefore, the traditional three steps for complete silver coating, including prior surface modification, seeding, and subsequent growing, were effectively integrated into one step. The experimental results exhibited that perfect SiO_2/Ag core/shell composite microspheres were successfully synthesized through optimizing the reaction parameters like the solvent ingredient, reducer, and the reaction temperature. Additionally, these obtained uniform composite microspheres were further used as SERS substrate by using R6G and thiram as probe molecules, and showed excellent trace detection of these organic chemicals in solution.

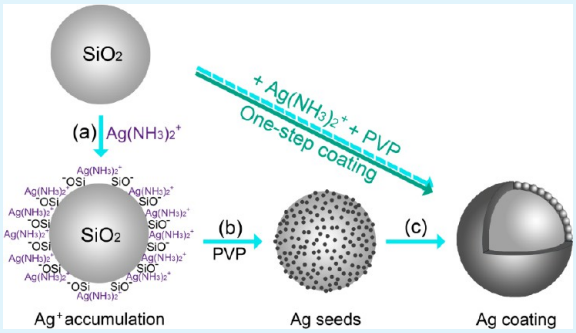

KEYWORDS: *silica colloidal spheres, silver coating, template-activated, SERS properties*

1. INTRODUCTION

The design and controlled fabrication of metal-coated core/shell composite microspheres have attracted many researchers' attention for their widely applications in various fields, such as nanoengineering of optical resonance,[1] surface-enhanced Raman scattering,[2] photonic crystals,[3] and catalysis,[4] etc. Great deals of efforts have been focused on preparing core/shell composite nanospheres with noble metallic shells such as Au and Ag because they exhibit novel optical properties,[5] and a variety of routes have been developed, including thermal evaporation,[6] hydrothermal method,[7] ultrasound irradiation,[8−10] layer-by-layer,[11] self-assembly,[12] solvent-assisted deposition methods,[13] electroless plating,[14,15] and so on.

The silica (SiO_2) colloidal microspheres, as the familiar and traditional core templates, are always the focus in the research field of core/shell materials, for they have many advantages including their narrow size distribution, simplicity of their well-known synthesis formulation, and ready availability both in large amounts and a wide range of sizes from commercial sources.[16] However, the direct coating on SiO_2 colloidal template was acknowledged to be difficult for the incompatibility between the template surface and shell materials, thus it became necessary to functionalize or modify the template with special functional groups or characteristics in order to increase the degree of surface coverage. And metal nanoparticles were often introduced onto SiO_2 colloidal microspheres by two avenues, including the in situ electroless plating of mental nanoparticles through Sn^{2+} modification and anchoring prefabricated metal nanoparticles after modification,[17−19] these nanometer-sized Ag or other metal particles attached on their surface favored for the subsequent seed growth. Lately, against the disadvantages in the previous methods like seeds impurity and complex surface modifications, Zhang et al put forward the combined solvent-assisted and electroless plating route, but the seeding step was also necessary before the shell coating.[13] Until now, although all kinds of methods were developed to coat metal around the colloidal template especially the SiO_2, the prior surface functionalization or modification on the core template was still the inevitable step for achieving uniform and complete metal coating.

It was noticed that the SiO_2 colloidal sphere in almost all the above methods was considered as physical template for its inertial property, and the chemical properties of SiO_2 colloidal microsphere were usually neglected, for example, some silicon−oxygen bonds on the surface of the SiO_2 colloidal spheres could be broken or form ionized sites (-SiO^- groups) in different alkaline conditions.[20−22] Although some researchers including our groups found the SiO_2 colloidal microspheres could attract silver ions in ammonia−water−ethanol mixed solution, only a few silver nanoparticles were coated around the silica colloidal

Received: November 13, 2013
Accepted: December 19, 2013
Published: December 19, 2013

microspheres.[23−25] Herein, on the basis of the above statements and our previous studies, we designed a template-activated strategy to realize one-step coating SiO_2 colloidal microspheres with sliver, where surface modification, seeding, and the subsequent shell growing steps could be achieved in one-pot hydrothermal reaction.

As illustration in the Scheme 1, the proposed intermediate growth processes were demonstrated: (a) As it was well-known

Scheme 1. Template-Activated Strategy Toward One-Step Coating SiO_2 Colloidal Microspheres with Silver

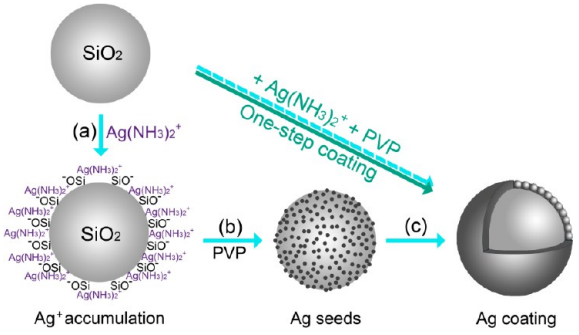

that the silanol groups (-Si−OH) at the surface of the silica colloidal microspheres are ionized by hydroxyl anions present in alkaline solution, which implies that a large surface charge will be present.[22] Therefore, in our experiment, the SiO_2 colloidal spheres then could be activated with negatively charged SiO^- groups in ammonia solution, which made the traditional surface functionalization like NH_2 groups or Sn^{2+} modification unnecessary.[26−28] Moreover, the number of functional groups on the surface of SiO_2 colloidal microspheres will not change once traditional surface modification was done. Here the functional SiO^- groups could be generated continually in ammonia solution. Thus, positive-charged complex ions $[Ag(NH_3)_2]^+$ or Ag^+ would be captured around the SiO_2 colloidal microspheres persistently in such system. (b) After some $[Ag(NH_3)_2]^+$ or Ag^+ ions were accumulated around the SiO_2 colloidal spheres, they were then gradually reduced by weak reducer, and generated silver nanoparticles as seeds in situ. Here PVP was specially chosen as reducer for its weak reducing and dispersing property, which will be discussed in detail in the following section. (c) The initial-generated Ag seeds acted as the growing center for the subsequent shell growth until complete silver coverage were realized. All the reaction steps mentioned above were integrated and achieved in one-pot hydrothermal reaction in our paper through optimizing the reaction system. The highlight or advantage of this method was that the SiO_2 colloidal microsphere as the core template was activated all through the reaction process, which avoided prior surface modification and seeding steps naturally, thus simplified the silver coating process to a great extent. The experiments indicated that optimal reaction conditions could be achieved to yield uniform and complete coverage Ag shell on SiO_2 colloidal microspheres reproducibly. Additionally, the surface-enhanced Raman spectroscopy (SERS) experimental results showed that these composite microspheres with Ag nanoparticle-assembled shells exhibited great potential for detecting trace of organic compounds with very high sensitivity in aqueous solutions.

2. EXPERIMENTAL SECTION

Materials. Tetraethoxysilane (TEOS, 99%), poly (vinyl pyrrolidone) (PVP, K30), ammonia (28%), ethanol (99.5%) and silver nitrate ($AgNO_3$, 99.5%) were purchased from Sinopharm Chemical Reagent Co., Ltd. All chemicals were of analytical grade and used without further purification.

2.1. Preparation of SiO_2/Ag Core/Shell Composite Microspheres. The SiO_2 colloidal microspheres used in our experiments were prepared by the Stöber method.[29] The stock solution was prepared by dispersing 1.5 g of SiO_2 colloidal microspheres in 30 mL of ethanol. In a typical Ag coating experiment, $AgNO_3$ (0.1 g) was first dissolved into water−ammonia solution (water 2 mL, ammonia 0.2 mL), and PVP (1 g) was added into ethanol solution (13 mL) containing SiO_2 colloidal microspheres (25 mg, through diluting 0.5 mL of the above stock solution). The above two solutions were then mixed together under magnetic stirring. After it was dispersed in an ultrasonic bath for several minutes, the mixed solution (15 mL) was transferred into a Teflon-lined stainless steel autoclave (20 mL) and heated at 120 °C for 12 h in an electric oven. After the autoclave was cooled naturally, and the product was taken out and centrifuged at a speed of 5000 rpm for 2 min, and then washed by ethanol, tetrahydrofuan, and deionized water for several times. The final product was saved in ethanol for further characterizations.

2.2. Characterizations. The morphology and composition of the as-prepared products were characterized by field-emission scanning electron microscopy (FESEM, Sirion 200 FEG) with an energy-dispersive X-ray spectrometer (EDS, Oxford, Link ISIS). Transmission electron microscopy (TEM) observations were performed on a JEOL 2010 electron microscope operating at 200 kV. The phase and the crystallographic structure of the products were investigated by X-ray diffraction (XRD, Philips X' Pert Pro). The elemental analysis was conducted by using inductively coupled plasma-atomic emission spectroscopy (ICP-AES). UV−vis absorption measurements were carried out using a Varian Cary 50 UV−visible spectrometer.

2.3. SERS Measurements. Rhodamine 6G (R6G) was used as Raman probes for the SERS measurements. During the SERS tests, the as-obtained SiO_2/Ag core/shell composite microspheres (about 35 mg) were first dispersed in 50 mL of solution as stock solution, and then 2 mL of that (about 0.7 mg) was dropped into R6G solutions (20 mL) with different concentrations for 1 h. After the products were centrifuged and rinsed with deionized water, they were dropped on glass slide substrate and dried under atmosphere. Finally, the glass slide substrate was characterized for Raman tests. Confocal microscopy Raman Spectrometer (LABRAM-HR) was used using a laser beam with an excitation wavelength of 514.5 nm in this study. The acquisition time was 3 s for each spectrum. The detecting tests of thiram in aqueous solution were conducted in a similar method.

3. RESULTS AND DISCUSSION

3.1. Characterization of Monodispersed SiO_2/Ag Core/Shell Composite Microspheres. The SiO_2 colloidal template and the final obtained composite SiO_2/Ag core/shell composite colloidal microspheres were first characterized by SEM and TEM. As shown in Figure 1a, monodispersed SiO_2 colloidal microspheres with 500 nm were first prepared according to Stöber method, and the SiO_2 microspheres were uniform with smooth surface. After silver coating, the microspheres were still uniform, but their surface became rough, which could be seen clearly from Figure 1b. Besides, the diameter of composite microspheres was estimated to be about 600 nm, larger than that of naked SiO_2 colloidal microspheres, indicating Ag shell with thickness of about 50 nm was coated successfully on SiO_2 colloidal microspheres. Magnified SEM image presented in Figure 1c further exhibited that the surface of the microspheres was obviously composed of nanoscaled Ag particles. By sampling nearly fifty nanoparticles on the shell of the composite microspheres in Figure 1c, the size of most of

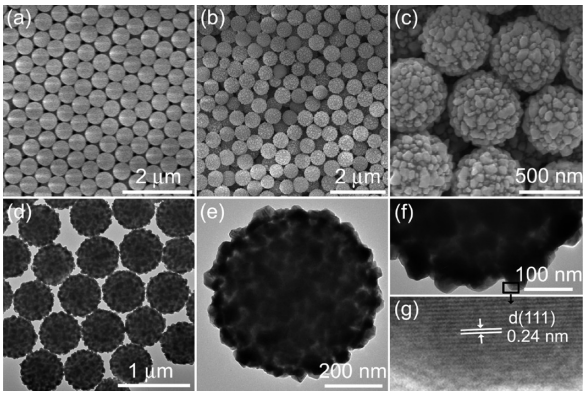

Figure 1. SEM images of (a) SiO_2 and (b) SiO_2/Ag core/shell composite microspheres; (c) magnified SEM image of SiO_2/Ag core/shell composite microspheres; TEM images of (d) SiO_2/Ag core/shell composite microspheres and (e) a single SiO_2/Ag core/shell composite microsphere; (f) magnified TEM image of partial SiO_2/Ag core/shell composite microsphere; (g) HRTEM image of the boxed region in f.

silver nanoparticles ranged from 40 to 70 nm. Through XRD characterizations, pure silver shell with face-centered cubic structure was identified from the peaks in Figure S1b in the Supporting Information (JCPDS no. 04−0783), and the peak around 23° could be indexed to amorphous silica from the SiO_2 core template characterized in Figure S1a in the Supporting Information.[30] To further investigate the structure of shell, we characterized the obtained samples by TEM. A strong contrast difference between the edges (dark) and center (gray) in Figure 1d was observed that is consistent with the SEM investigation, implying that the SiO_2/Ag core/shell composite microspheres were synthesized. The spike-like nanoparticles and the gaps between them were clearly observed from the magnified edge of the shell in Figure 1f. The further magnified image of the nanoparticle marked by rectangle showed clear lattice fringes (Figure 1g), and the indexed fringe spacing of 0.24 nm was consistent with the interplanar distance of the (111) planes of cubic silver structure.

3.2. Influence of the Reaction Parameters on Silver Coating. The above results clearly indicated that SiO_2/Ag core/shell composite microspheres were successfully obtained by our template-activated strategy. Because the coating was achieved in one step rather than traditional three steps, the reaction factors needed to be carefully controlled, and it was indeed found that the morphology and structure of products were strongly influenced by the reaction conditions. As mentioned in Scheme 1, two critical aspects should be specially paid attention in the reaction process, including (1) the surface of SiO_2 colloidal microspheres was activated to be negatively charged with SiO^- in ammonia solution for accumulating silver ions, rather than the dissolution of SiO_2 template, thus the gradient of reaction solution needed to be investigated in detail; (2) the reducer should guarantee that the silver ions were mainly reduced and generated around the SiO_2 colloidal microspheres rather than homogeneous nucleation in solution, thus the proper kind of reducer should be selected. Besides, the reaction temperature also indirectly affected the above two aspects. Therefore, reaction conditions should be optimized carefully in the present system. In the following, the influences of main reaction factors including solvent gradient, the reducer, and reaction temperature were investigated, respectively.

$$NH_3 + H_2O \rightarrow NH_4^+ + OH^- \quad (1)$$

$$(\text{amorphous})nSiO_2 + OH^- \rightarrow nSiO^- + H_2O \quad (2)$$

3.2.1. Effect of Solvent Ingredient on the Morphology of Products. The surface silicon−oxygen bonds of SiO_2 colloidal microspheres could be broken by hydroxyl ions through the hydrolysis of ammonia according to eqs 1 and 2.[22] In the designed hydrothermal reaction, both ammonia and water were requisite reagents to activate the surface of SiO_2 colloidal microspheres with SiO^- groups for the following attraction of silver ions, but their amounts should be as few as possible to avoid the dissolution of SiO_2 colloidal microspheres. For ammonia, here only 0.2 mL was used into silver solution, which was just full enough to complex with silver ions to form a clear solution. As for water, it also promoted the breaking of silicon−oxygen bonds through the hydrolysis of ammonia, but over amount of water could arouse fast breaking of silicon−oxygen bonds and dissolution of SiO_2, thus the proper amount of water should be adjusted. Here ethanol was used as major solvent to restrain the fast breaking of silicon−oxygen bonds, and the water content in the solvent which was critical to the generation of SiO^- groups for accumulation of silver ions was discussed. Serial experiments with different volume ratio of water and ethanol (W/E) were conducted while keeping the other conditions unchanged. Figure 2 showed the SEM images of

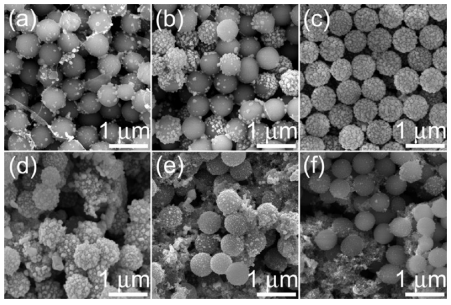

Figure 2. SEM images of products synthesized with different volume ratio of water/ethanol: (a) 0:15, (b) 1:14, (c) 2.5:12.5, (d) 4:11, (e) 9:6, and (f) 15:0.

silver nanostructures synthesized at different W/E (Note: here the water from ammonia was not calculated). When no water (W/E = 0:15) was introduced into the solution, only few silver particles were observed on the surface of SiO_2 colloidal microspheres in Figure 2a. Through increasing W/E to 1:14, the silver nanoparticles around the surface of SiO_2 colloidal microspheres became more, but still not enough for full cover in Figure 2b. Then, we carefully adjusted the volume ratio W/E to 2.5:12.5, and the microspheres with perfect coating were observed in Figure 2c. However, if we continually increase the content of water in solvent (W/E = 4:11), the silver coating became poor again on SiO_2 colloidal microspheres and separate silver nanoparticles appeared in Figure 2d. When the ratio increased to 9:6, large amount of separate silver nanoparticles were observed, and only few silver particles were attached on the SiO_2 colloidal microspheres in Figure 2e. Especially, when the solvent with W/E = 15:0 were used, almost all the SiO_2 colloidal microspheres were naked with sparsely distributed silver nanoparticles, and the SiO_2 colloidal microspheres also seemed to be smaller seen in Figure 2f. Through the above experiments, the water affected the morphology of the final product seriously, and neither little water (0:15 and 1:14) nor

excessive water (9:6 and 15:0) in the solvent could guarantee full shell coating. The reason was proposed as we stated above that the water impacted the attracting and reducing of silver ions through influencing the density SiO^- groups around SiO_2 colloidal microspheres, little water could not provide enough SiO^- groups for substantive accumulation of silver ions, while excessive water dissolved the SiO_2 colloidal microspheres which also could not capture and hold silver ions nearby the SiO_2 template.

The silicon element in the solution maybe indirectly reflected the dissolution degree of SiO_2 colloidal microspheres and thus verified the above proposition. Here the silicon (Si) element in the solutions of the above six products were studied, and the concentrations of Si element in different reaction conditions were summed as shown in Table S1 in the Supporting Information. The concentrations of Si element were found to increase rapidly with the increasing amount of water, especially when the W/E was above 2.5:12.5. For example, the Si element in the solution (W/E = 15:0) is more than fourteen times of that in the solution (W/E = 2.5:12.5). These revealed that silicon−oxygen bonds at the surface of SiO_2 colloidal microspheres were seriously broken forming SiO_4^- ions in solution at high W/E ratio,[31] whereas only partial Si−O bonds were broken, forming SiO^- groups at low W/E. Therefore, the amount of water in reaction solution was critical for the generation of SiO^- groups, which then influenced the generation of silver seeds and the final morphology of products.

3.2.2. Effect of Reducer PVP on the Morphology of Products. As we mentioned above, the reducer should be satisfied that the silver ions were reduced around the SiO_2 colloidal microspheres rather than homogeneous nucleation in solution, for silver seeds around the SiO_2 colloidal microspheres were very important for subsequent shell growth. Several common reducers were adopted, for example, ascorbic acid (AA), a kind of moderate reducer, was used in the reaction system; however, the silver ions were found to be reduced at room temperature quickly from the color change of the solution from white to gray, and large separated silver particles were generated rather than deposited onto the surface of SiO_2 colloidal microspheres seen in Figure S2 in the Supporting Information. Obviously, here the unsuccessful silver coating was that the silver ions in the solution were easily reduced even it coupled with ammonia in solution. Thus no silver nanoparticles were generated around the SiO_2 colloidal microspheres, which meant no silver seeds existed for shell growing. Then the citrate, a rather weaker reducer than AA, was tried. Although no reaction happened at room temperature, only few silver nanoparticles were found on the surface of SiO_2 colloidal microspheres after hydrothermal reaction in Figure S3 in the Supporting Information. Obviously, the reducing capability of citrate ions was still too high, because the reduction reaction mainly preceded in solution phase rather the surface of SiO_2 colloidal microspheres, and then the silver shell growing could not predominate in such reaction system.

PVP, a kind of non-ionic polymer, was widely used as dispersant in the preparation of stable colloidal solutions of metal nanoparticles (NPs) including Ag, Au, and Pt. However, it was found that the PVP could reduce silver ions in water solution recently, where the reducing capability of PVP was proposed to arise from its hydroxyl end-group.[32−34] When PVP was chosen as reducer in our experiment, most of silver ions were deposited around the SiO_2 colloidal microspheres seen in Figure 1b. Therefore, PVP was a proper reducer in our experiment for complete silver coating. Obviously, the amount of PVP influenced the reaction process as shown in Figure 3,

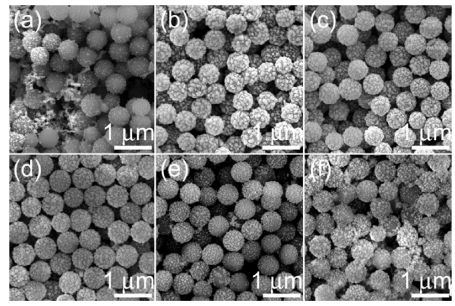

Figure 3. SEM images of products synthesized with different amounts of PVP (g): (a) 0, (b) 0.05, (c) 0.2, (d) 1, (e) 1.5, and (f) 2.

when no PVP were used, only few silver nanoparticles were observed on the surface of SiO_2 colloidal microspheres in Figure 3a, which could be primarily ascribed to the solvent ethanol. When the amount of PVP was above 0.05 g, complete shell coating were realized in Figure 3b−d. By comparing these shells, the sizes of silver nanoparticles around the SiO_2 colloidal microspheres were clearly different in these three products, where nanoparticles on the shell became smaller in turn with the increasing amount of PVP from 0.05 to 1 g. It may be ascribed to the restriction effect of PVP during the growing process, since it could be adsorbed on the surface of silver nanoparticles. However, when more PVP weas used, incomplete shell coating was found again in both images e and f in Figure 3. We noticed that the precursor solution became sticky with 1 g or more PVP, and the excessive PVP molecules were proposed to block the diffusion of silver ions onto the surface of SiO_2 colloidal microspheres, and then affected the growing of silver shell. To sum up, the amount of PVP should be adjusted ranging from 0.05 to 1 g for complete silver shell coating.

3.2.3. Effect of Reaction Temperature on the Morphology of Products. The products at different temperatures were studied from 80 to 140 °C for optimal conditions. As shown in Figure 4a, the product synthesized at 80 °C exhibited some naked or sparsely silver nanoparticles decorated SiO_2 colloidal microspheres. When the temperature increased to 100 °C, more silver nanoparticles were observed on the surface of SiO_2 colloidal microspheres, indicating more silver ions were reduced with increasing temperature in Figure 4b. The SiO_2 colloidal microspheres were full covered by silver nanoparticles

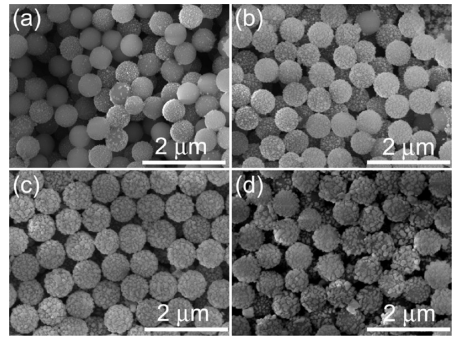

Figure 4. SEM images of products synthesized with different temperatures (°C): (a) 80, (b) 100, (c) 120, and (d) 140.

when the reaction system was heated at 120 °C in Figure 4c. However, the coverage became poor again at 140 °C in Figure 4d, and partial surface of SiO_2 colloidal microspheres emerged. In our system, the reaction temperature was proposed to influence the reducing capability of PVP and the growth rate of silver, which became stronger and faster with increasing temperature. Therefore, when low temperature was used, silver ions were reduced too slowly; when high temperature was applied, the reduction rate increased rapidly, and homogeneous nucleation became active which decreased the supply of silver ions to the shell growing, thus incomplete shell coating was found in Figure 4d.

3.3. Growth Process of SiO_2/Ag Core/Shell Composite Microspheres. Through the above investigation and discussion, optimal parameters were obtained by investigating the reaction conditions in detail. Here the time-depended products at optimal parameters were observed to validate the growth mechanism. By immersing the SiO_2 microspheres in ethanol containing ammonia and silver ions for 1 h, peaks of silver element could be observed from EDX spectrum in Figure S4, which indicated that silver ions were indeed adsorbed onto the surface of colloidal microspheres at the beginning of the experiment. The products sampled from 1 to 10 h were then characterized and demonstrated in Figure 5. At 1 h, the SiO_2 colloidal microsphere were decorated by large amount of silver nanoparticles, as seen clearly in Figure 5a and e, which indicated the successfully accumulation and reduction of silver ions around SiO_2 template in the designed system. These tiny silver nanoparticles became denser after 2 h's reaction in Figure 5b and f. Obviously, these new-generated tiny silver nanoparticles played as seeds for the subsequent silver shell growth, which grow larger and became denser at 4 h in Figure 5c and g. After 10 h of growing, the SiO_2 microspheres were finally covered with complete Ag shell in Figure 5d and h. From the whole reaction process, the coating procedure corresponded with the illustration in Scheme 1. Compared with traditional methods, the prior surface functionalization of SiO_2 colloidal microspheres was replaced by negative-charged SiO^- groups generated through self-activation of SiO_2 colloidal microspheres in ammonia solution, and then the silver ions were attracted around the SiO_2 colloidal microspheres and reduced into silver nanoparticles in situ as seeds, thereafter the seeds continued to grow until a complete shell was achieved. It could be concluded that the traditional three-step coating process including surface modification, seeding, and growing was effectively integrated into one step through template-activated strategy in our experiment, which simplified the whole coating process greatly. Additionally, the SiO_2/Ag core/shell composite microspheres with thicker Ag shell could be easily obtained by increasing silver concentrations through the above strategy as shown in Figure S5 in the Supporting Information.

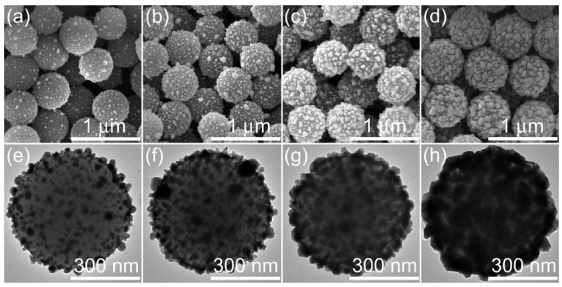

Figure 5. SEM images of the products obtained at different intervals (h): (a) 1, (b) 2, (c) 4, and (d) 10, and (e–h) their corresponding TEM images.

3.4. Optical Properties of the Products. The UV–vis adsorption spectra were used to investigate the silver shell coating process at different stages. All the products were diluted with deionized water for the measurement of adsorption spectrum. As shown in Figure S6 in the Supporting Information, the bare silica colloidal microspheres exhibited no adsorption peaks in curve a, and the absorption just increases with decreasing wavelength. A broad hump around 480 nm appears in curve b for the product synthesized at 1 h, which could be attributed to the plasmon resonance of Ag nanoparticles generated on the surface of silica colloidal microspheres. When the silver thickness and coverage are increased through subsequent growth, the silver nanoparticles grow larger and eventually coalesce together, and the plasmon peak broadens and red shifts from curve b to e. The red shift of the peaks could be caused by the dipole–dipole interaction among silver nanoparticles deposited on the dielectric cores, where the electromagnetic coupling may enhance the polarizability of the electron cloud to lower the plasmon resonance energy and resulting in the red shift of SPR. This interaction also contributes to the enhancement of local electric field between silver nanoparticles.[35]

3.5. SERS Property of Uniform SiO_2/Ag Core/Shell Composite Microspheres. Recent advances in SERS allowed dramatic signal enhancement for analyte adsorbed on Au or Ag nanostructured materials.[36] When fundamental understanding of the mechanism of the enhancement was emerging, the preparation of highly consistent SERS substrate with high enhancement factor became an active research area.[37] It has been observed that the aggregated Ag or Au particles give the high enhancement, which is postulated to be the coupling of the plasmon resonance of the nearby particles with the strongest field enhancement between them, calling "hot spots".[38] Here in our product, the size of silver nanoparticles ranging from 40 to 70 nm aggregated around the SiO_2 microspheres, which formed plenty of gaps or apertures in the shell, which would be suitably for SERS substrate.[39] Rhodamine 6G (R6G), a cationic dye, was chosen in this study because of its active role in surface-enhanced Raman spectroscopy (SERS), and we found the zeta potential of final product was negative (−30 mV), thus R6G molecules could interact with silver nanoparticles through their amino group (Ag–N).[40−42] Figure 6 showed the SERS spectrum with a concentration of 1×10^{-12} M on the substrate. All peaks ranging from 400 to 1800 cm^{-1} are characteristic peaks of R6G. For example, vibrations at 1187, 1311, 1363, 1509, and 1651 cm^{-1}, which are assigned to C–H in-plane bending, C–O–C stretching, and C–C stretching of the aromatic ring, and the peak at 773 cm^{-1} is due to the out-of-plane bending motion of the hydrogen atoms of the xanthene skeleton.[41] Although the concentration of R6G was very low (1×10^{-12} M), the signals of the SERS were still strong. The SERS enhancement factors (EF) for R6G on the SiO_2/Ag composite microspheres can be calculated according to the equation.[43]

$$EF = (I_{SERS}/I_{bulk})(N_{bulk}/N_{ads})$$

where N_{bulk} is the number of analyte molecules in the focal volume and I_{bulk} is the intensity of the Raman signal as calculated from the main peak area, whereas N_{ads} and I_{SERS} are the same parameters when the SERS substrate is utilized. In the

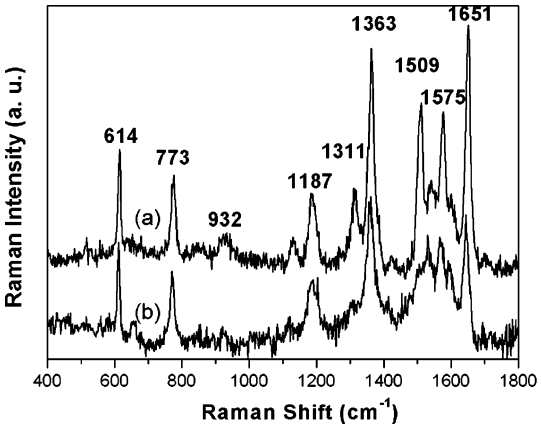

Figure 6. (a) SERS spectrum of R6G adsorbed on SiO_2/Ag composite microspheres with concentrations of 1×10^{-12} M (20 mL) and (b) normal Raman spectrum of R6G with concentrations of 1×10^{-2} M (20 μL).

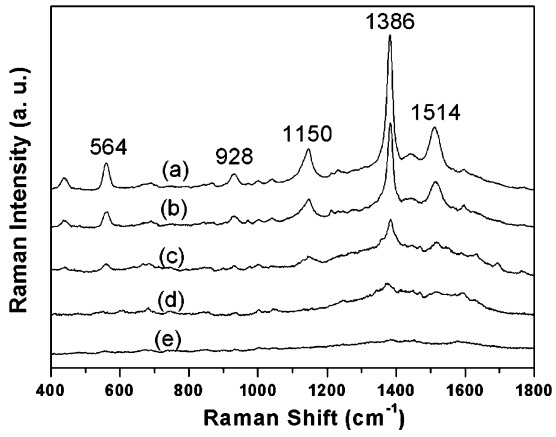

Figure 7. SERS spectra of thiram adsorbed on SiO_2/Ag composite microspheres with different concentrations: (a) 1×10^{-5} M, (b) 1×10^{-6} M, (c) 1×10^{-7} M, (d) 1×10^{-8} M, and (e) 1×10^{-9} M.

present experiment, the 20 μL R6G solution (1×10^{-2} M) and the R6G-absorbed SiO_2/Ag composite microspheres (separated from the R6G solution 1×10^{-12} M, 20 mL) were spread on a bare glass slide with the same area uniformly. We assume that all the R6G molecules are adsorbed on SiO_2/Ag composite microspheres from the R6G solution, and all molecules contribute to the measured Raman signals within the laser spot area. Correspondingly, the ratio N_{bulk}/N_{ads} was calculated to be 1×10^7 within the same area of the laser spot. Meanwhile, the ratio I_{SERS}/I_{bulk} is about 1.68 for the vibrational peak at 1363 cm^{-1} in curve a and b (Figure 6), thus the EF value is calculated to be about 1.68×10^7. These results indicated that the synthesized SiO_2/Ag core/shell composite microspheres were effective and ultrasensitive when used as SERS substrate for trace detection.

Rapid detection and identification of poisonous substances in water or aqua environment is one of the most important tasks for SERS analysis.[44] For a practical application, the SiO_2/Ag core/shell composite microspheres were also used as SERS substrate for pesticide analysis. As we know, pesticides are annually used to control pests of agriculture and forestry while they may cause problems of environmental pollution and also residues. For example, the thiram, a member of the dithiocarbamate family, could lead to serious skin and eye illnesses, as well as damage to the liver due to the carbon disulfide release from thiram.[45] Thus developing an accurate and rapid detection method is a very important and significant task. Due to its ultrahigh sensitivity and "fingerprint-like" property, SERS exhibited a great advantage for the detection of thiram recently. Here monodispersed SiO_2/Ag core/shell composite microspheres were used as SERS substrate to investigate the detection of thiram, and the corresponding SERS spectra at different concentrations from 1×10^{-5} to 1×10^{-9} M were obtained as shown in Figure 7. All the peaks from 400 to 1800 cm^{-1} in curve a are attributed to thiram signals according to previous reports,[46,47] where the main Raman bands could be assigned as following, 564 cm^{-1} attributed to υ_s(CSS), 928 cm^{-1} to $\upsilon(CH_3N)$ or υ(C−S), 1150 cm^{-1} to $\rho(CH_3)$ or υ(C−N), and 1386 and 1514 cm^{-1} to $\rho(CH_3)$ or υ(C−N), respectively. All feature peaks of thiram band could be clearly observed even at the low level of 10^{-7} M in Figure 7c. Figure S7 in the Supporting Information reflects the relationship between SERS intensity at 1386 cm^{-1} and the concentrations of the thiram in water, and the signals of thiram can easily be noticed even at the 1×10^{-8} M level in Figure 7d. These results indicated that the present product exhibited a high sensing ability for thiram and could be applied for the trace detection of thiram in water.

4. CONCLUSION

In summary, we presented a template-activated strategy toward uniform coating silver on the traditional SiO_2 colloidal microspheres in one step, which greatly simplified the traditional coating process. The influences of factors like solvent, reducer and reaction temperature were closely discussed, and the time-depended experiments also validated the designed strategy. This strategy may provide a simple avenue for other metal deposition around silica colloidal microspheres. The uniform SiO_2/Ag core/shell composite microspheres were also investigated as SERS substrate, which demonstrated an excellent detecting performance to R6G and thiram.

■ ASSOCIATED CONTENT

Supporting Information

XRD spectra, EDX spectrum, SEM images, TEM images, UV−vis adsorption spectra, and table for elemental analysis of the corresponding products. This material is available free of charge via the Internet at http://pubs.acs.org.

■ AUTHOR INFORMATION

Corresponding Author

*E-mail: wangyq@henu.edu.cn.

Notes

The authors declare no competing financial interest.

■ ACKNOWLEDGMENTS

This work was supported by the Natural Science Foundation of China (51102077 and 51372070), the Doctoral Scientific Research Foundation of Henan University (B2010088), and Changjiang Scholars and Innovative Research Team in University (PCS IRT1126).

■ REFERENCES

(1) Jackson, J. B.; Halas, N. J. *J. Phys. Chem. B* **2001**, *105*, 2743−2746.

(2) Li, J.; Ma, W.; Wei, C.; You, L.; Guo, J.; Hu, J.; Wang, C. *Langmuir* **2011**, *27*, 14539−14544.
(3) Zhang, W. Y.; Lei, X. Y.; Wang, Z. L.; Zheng, D. G.; Tam, W. Y.; Chan, C. T.; Sheng, P. *Phys. Rev. Lett.* **2000**, *84*, 2853−2856.
(4) Ataee-Esfahani, H.; Nemoto, Y.; Wang, L.; Yamauchi, Y. *Chem. Commun.* **2011**, *47*, 3885−3887.
(5) Kim, J. H.; Bryan, W. W.; Lee, T. R. *Langmuir* **2008**, *24*, 11147−11152.
(6) Schueler, P. A.; Ives, J. T.; DeLaCroix, F.; Lacy, W. B.; Becker, P. A.; Li, J.; Caldwell, K. D.; Drake, B.; Harris, J. M. *Anal. Chem.* **1993**, *65*, 3177−3186.
(7) Song, C. X.; Wang, D. B.; Lin, Y. S.; Hu, Z. S.; Gu, G. H.; Fu, X. *Nanotechnology* **2004**, *15*, 962−965.
(8) Ye, X. Y.; Zhou, Y. M.; Chen, J.; Sun, Y. Q. *Appl. Surf. Sci.* **2007**, *253*, 6264−6267.
(9) Pol, V. G.; Srivastava, D. N.; Palchik, O.; Palchik, V.; Slifkin, M. A.; Weiss, A. M.; Gedanken, A. *Langmuir* **2002**, *18*, 3352−3357.
(10) Ye, X. Y.; Cai, S. G.; Zheng, C.; Xiao, X. Q. *Adv. Mater. Res.* **2012**, *479*, 541−545.
(11) Dong, A. G.; Wang, Y. J.; Tang, Y.; Ren, N.; Yang, W. L.; Gao, Z. *Chem. Commun.* **2002**, *4*, 350−351.
(12) Sadtler, B.; Wei, A. *Chem. Commun.* **2002**, *15*, 1604−1605.
(13) Zhang, J. H.; Liu, J. B.; Wang, S. Z.; Zhan, P.; Wang, Z. L.; Ming, N. B. *Adv. Funct. Mater.* **2004**, *14*, 1089−1096.
(14) Liu, J. B.; Dong, W.; Zhan, P.; Wang, S. Z.; Zhang, J. H.; Wang, Z. L. *Langmuir* **2005**, *21*, 1683−1686.
(15) Kobayashi, Y.; Salgueirino-Maceira, V.; Liz-Marzan, L. M. *Chem. Mater.* **2001**, *13*, 1630−1633.
(16) Lou, X. W.; Archer, L. A.; Yang, Z. C. *Adv. Mater.* **2008**, *20*, 3987−4019.
(17) Kim, J.; Bryan, W. W.; Chung, H.; Park, C. Y.; Jacobson, A. J.; Lee, T. R. *ACS Appl. Mater. Interfaces* **2009**, *1*, 1063−1069.
(18) Liu, T.; Li, D.; Yang, D.; Jiang, M. *Chem. Commun.* **2011**, *47*, 5169−5171.
(19) Liu, T.; Li, D.; Yang, D.; Jiang, M. *Colloids Surf., A* **2011**, *387*, 17−22.
(20) Ren, N.; Wang, B.; Yang, Y. H.; Zhang, Y. H.; Yang, W. L.; Yue, Y. H.; Gao, Z.; Tang, Y. *Chem. Mater.* **2005**, *17*, 2582−2587.
(21) Wang, Y. Q.; Zou, B. F.; Li, G. H.; Zhou, S. M. *Mater. Lett.* **2011**, *65*, 1601−1604.
(22) Bergna, H. E. Roberts, W. O. *Colloidal Silica: Fundamentals and Applications*; CRC Press: New York, 2005; pp 559−600.
(23) Deng, Z. W.; Chen, M.; Wu, L. M. *J. Phys. Chem. C* **2007**, *111*, 11692−11698.
(24) Wang, Y. Q.; Wang, K.; Zou, B. F.; Gao, T.; Zhang, X. L.; Du, Z. L.; Zhou, S. M. *J. Mater. Chem. C* **2013**, *1*, 2441−2447.
(25) Chen, K.; Pu, Y.; Chang, K.; Liang, Y.; Liu, C.; Yeh, J.; Shih, H. C.; Hsu, Y. *J. Phys. Chem. C* **2012**, *116*, 19039−19045.
(26) Jiang, Z.; Liu, C. *J. Phys. Chem. B* **2003**, *107*, 12411−12415.
(27) Kim, S. W.; Kim, M.; Lee, W. Y.; Hyeon, T. *J. Am. Chem. Soc.* **2002**, *124*, 7642−7643.
(28) Xiu, Z.; Wu, Y.; Hao, X.; Zhang, L. *Colloids Surf., A* **2011**, *386*, 135−140.
(29) St, W.; Fink, A. *J. Colloid Interface Sci.* **1968**, *26*, 62−69.
(30) Wang, Y. Q.; Wang, G. Z.; Wang, H. Q.; Cai, W. P.; Liang, C. H.; Zhang, L. *Nanotechnology* **2009**, *20*, 155604−155609.
(31) Wang, Y. Q.; Wang, G. Z.; Wang, H. Q.; Liang, C. H.; Cai, W. P.; Zhang, L. D. *Chem.—Eur. J.* **2010**, *16*, 3497−3503.
(32) Washio, I.; Xiong, Y.; Yin, Y.; Xia, Y. *Adv. Mater.* **2006**, *18*, 1745−1749.
(33) Xiong, Y.; Washio, I.; Chen, J.; Cai, H.; Li, Z.; Xia, Y. *Langmuir* **2006**, *22*, 8563−8570.
(34) Xia, X.; Zeng, J.; Oetjen, L. K.; Li, Q.; Xia, Y. *J. Am. Chem. Soc.* **2012**, *134*, 1793−1801.
(35) Chen, D.; Liu, H.; Liu, J.; Ren, X.; Meng, X.; Wu, W.; Tang, F. *Thin Solid Films* **2008**, *516*, 6371−6376.
(36) Moskovits, M. *Rev. Mod. Phys.* **1985**, *57*, 783−826.
(37) Smith, W. E. *Chem. Soc. Rev.* **2008**, *37*, 955−964.
(38) Kleinman, S. L.; Frontiera, R. R.; Henry, A.; Dieringer, J. A.; Van Duyne, R. P. *Phys. Chem. Chem. Phys.* **2013**, *15*, 21−36.
(39) Stamplecoskie, K. G.; Scaiano, J. C.; Tiwari, V. S.; Anis, H. *J. Phys. Chem. C* **2011**, *115*, 1403−1409.
(40) Watanabe, H.; Hayazawa, N.; Inouye, Y.; Kawata, S. *J. Phys. Chem. B* **2005**, *109*, 5012−5020.
(41) Hildebrandt, P.; Stockburger, M. *J. Phys. Chem.* **1984**, *88*, 5935−5944.
(42) Zhao, J.; Jensen, L.; Sung, J.; Zou, S.; Schatz, G. C.; Duyne, R. P. *J. Am. Chem. Soc.* **2007**, *129*, 7647−7656.
(43) Le Ru, E. C.; Blackie, E.; Meyer, M.; Etchegoin, P. G. *J. Phys. Chem. C* **2007**, *111*, 13794−13803.
(44) Halvorson, R. A.; Vikesland, P. J. *Environ. Sci. Technol.* **2010**, *44*, 7749−7755.
(45) Liu, B.; Han, G.; Zhang, Z.; Liu, R.; Jiang, C.; Wang, S.; Han, M. *Anal. Chem.* **2011**, *84*, 255−261.
(46) Kang, J. S.; Hwang, S. Y.; Lee, C. J.; Lee, M. S. *Bull. Korean Chem. Soc.* **2002**, *23*, 1604−1610.
(47) Sánchez-Cortés, S.; Vasina, M.; Francioso, O.; García-Ramos, J. V. *Vib. Spectrosc.* **1998**, *17*, 133−144.